NONLINEAR PYRAMIDAL IMAGE DECOMPOSITIONS BASED ON LOCAL CONTRAST PARAMETERS

Pierre Vandergheynst and Ömer Nezih Gerek

Signal Processing Laboratory
Swiss Federal Institute of Technology
CH-1015, Lausanne, Switzerland
Pierre.Vandergheynst@epfl.ch
Omer.Gerek@epfl.ch

ABSTRACT

The 2-D pyramidal image decomposition has been widely used in various image processing applications [6]. In this paper, we introduce filter bank implementations of a nonlinear multiresolution image representation based on local contrast measure. Following the work of Duval-Destin [3, 1] for visual contrast sensitivity, we define multiscale contrast coefficients by scaling the wavelet transform with a localized mean luminance. We show that a pyramidal representation is naturally associated with this new set of coefficients and study its properties. As an application, preliminary results of image coding experiments are discussed.

1. INTRODUCTION

Relying on common psycho-visual tests indicates that our visual system is contrast sensitive, i.e. it reacts to the relative variations of the image intensity according to the celebrated Weber law [1] :

$$C = \frac{\Delta L}{L} .$$

On the other hand, the 2-D Continuous Wavelet Transform (CWT) is by now a well established tool to detect and characterize the absolute variations of the image intensity [2]. Using these basic definitions and properties, several authors [1, 7] have proposed to define a local measure of contrast by introducing an adaptive normalization of the CWT which would take into account the local luminance around the pixel of interest.

We will set up the contrast scaled version of the wavelet pyramid in the following manner. Let $h \in L^1(\mathbb{R}^2) \cap L^2(\mathbb{R}^2)$ be a real, positive valued function and ψ be a square-integrable 2-d wavelet. To avoid directional sensitivity, h and the wavelet ψ are taken isotropic. The intensity level of the image s around the position $\vec{b}$ is defined as:

$$\tilde{M}_s(a, \vec{b}) = \|h\|_1^{-1} \int_{\mathbb{R}^2} d^2\vec{x}\, s(\vec{x}) \tilde{h}_{a,\vec{b}}(\vec{x}) , \qquad (1)$$

where $\tilde{h}_{a,\vec{b}}(\vec{x}) = a^{-2} h(a^{-1}(\vec{x} - \vec{b}))$. In this expression, the image and the normalization function are positive, so $\tilde{M}_s$ is also positive and

$$\int_{\mathbb{R}^2} d^2\vec{b}\, \tilde{M}_s(a, \vec{b}) = \|s\|_1 .$$

As a result, $\tilde{M}_s$ plays the role of a local mean of s. The ratio of the wavelet coefficient at scale a and position $\vec{b}$ to the mean intensity level yields the following function :

$$C_s(a, \vec{b}) = \frac{\langle \tilde{\psi}_{a,\vec{b}} | s \rangle}{\tilde{M}_s(a, \vec{b})} . \qquad (2)$$

An important point is that, $C_s(a, \vec{b})$ is well defined for all $a \in \mathbb{R}_*^+$ and $\vec{b} \in \mathbb{R}^2$, if and only if the essential support of the wavelet is included in the corresponding support of the normalization function h. With this condition and by positivity of h and s,

$$\tilde{M}_s(a, \vec{b}) = 0 \;\; \Rightarrow \;\; C_s(a, \vec{b}) = 0.$$

In general, the positivity conditions can even be relaxed, provided one controls the zeros of the denominator of $C_s(a, \vec{b})$ in Eq. 2. This can be done by imposing analyticity of $\tilde{M}_s(a, \vec{b})$ [3]. At this point, $C_s(a, \vec{b})$ is called the local contrast of the image s around $\vec{b}$ at scale a [1]. It can be observed that C_s takes its large values in regions of low luminance. Perception-wise, this means that the details in dark areas are emphasized more than the details in the bright areas. This is essentially how the human visual system works, as well. If the adaptation of the human eye pupil function

[1] In fact there is no unique definition of contrast. Weber's law, for example, is commonly accepted when measuring the contrast with respect to a somewhat uniform background, but other definitions can be found in the literature [5].

is not considered, which is the case when both bright and dark regions exist in the same image, human visual system is more sensitive to variations in the dark regions that those in bright regions.

A nice simplification arises when the wavelet ψ is taken as a difference of two positive functions [4],

$$\psi(\vec{x}) = \alpha^{-2} h(\alpha^{-1}\vec{x}) - h(\vec{x}) \ (0 < \alpha < 1).$$

The function ψ satisfies the admissibility condition of wavelets [1] if the first moment of h vanishes at the origin. Taking the same function to compute the luminance, we have

$$C_s(a, \vec{b}) = \frac{\langle \tilde{\psi}_{a,\vec{b}} | s \rangle}{\langle \tilde{h}_{a,\vec{b}} | s \rangle} = \frac{\langle \tilde{h}_{a\alpha,\vec{b}} | s \rangle}{\langle \tilde{h}_{a,\vec{b}} | s \rangle} - 1 \qquad (3)$$

In this way, the support condition imposed on the wavelet turns into a constraint on h alone:

$$\text{Supp}\left(\tilde{h}_\alpha\right) \subseteq \text{Supp}\left(\tilde{h}_1\right) ,$$

which means that the support of h is a star-shaped domain around the origin. Notice that it is sufficient that h decays radially for C_s to be bounded.

Using this simple example, it is very easy to realize that the contrast coefficients yield a complete representation of the signal. In fact the reconstruction at a fixed resolution is a simple scheme using difference wavelets and local contrast. If a_0 is the finest resolution (scale), that is, $\tilde{M}_s(a_0, \vec{b})$ is the original dataset, and $\tilde{M}_s(a, \vec{b})$ is a low resolution approximation of the image with $a_0 = a\alpha^n$, $\alpha < 1$, then we have

$$\begin{aligned} \tilde{M}_s(a\alpha, \vec{b}) &= \tilde{M}_s(a, \vec{b}) \cdot \left(C_s(a, \vec{b}) + 1\right) \\ \tilde{M}_s(a\alpha^2, \vec{b}) &= \tilde{M}_s(a, \vec{b}) \cdot \left(C_s(a, \vec{b}) + 1\right) \\ &\quad \times \left(C_s(a\alpha, \vec{b}) + 1\right) . \end{aligned}$$

By recursion, a multiplicative reconstruction formula is obtained:

$$\tilde{M}_s(a_0\alpha, \vec{b}) = \tilde{M}_s(a, \vec{b}) \prod_{i=0}^{n-1} \left(C_s(a\alpha^i, \vec{b}) + 1\right) . \qquad (4)$$

This means that the reconstruction is obtained by starting from low resolution approximations and adding successive details, exactly like in the wavelet case.

The main difference is that the overall decomposition / reconstruction scheme is now a nonlinear operation in the sense that every decomposition value is adaptatively normalized, and the reconstruction operations require successive multiplications of the C functional where the regular wavelet reconstruction procedure requires additions. In other words, the regular wavelet synthesis works with a summation over the filtered approximation and detail signals, whereas, with the introduction of a scaling with the mean luminance values at each decomposition level, the local contrast wavelet reconstruction procedure works with a multiplication over the wavelet data.

2. PYRAMIDAL CONTRAST REPRESENTATIONS

Equation (4) shows us that contrast coefficients adopt a natural multiresolution structure allowing a coarse to grain representation of images. This close link with wavelets can also be exploited to design fast decomposition algorithm based on filter banks.

2.1. Laplacian Pyramid Style

In order to obtain a useful and less redundant representation, the CWT formalism is carried to the Discrete Wavelet Transform framework by introducing downsampling on the low resolution approximation. The easiest way to achieve this is to adapt the well known Laplacian Pyramid formalism [6]. In this scheme, the image I is first convolved with a low pass filter $K(i,j)$ and the result is downsampled by a factor of 2, yielding a low resolution approximation $L_1(i,j)$. In order to record the details lost in this operation we upsample L_1, interpolate with K and compute the difference image :

$$D_1(i,j) = I(i,j) - [L_1 \uparrow 2] \star K(i,j) .$$

Contrast coefficients are then defined as

$$C_1(i,j) = \frac{D_1(i,j)}{[L_1 \uparrow 2] \star K(i,j)} , \qquad (5)$$

which is obviously well defined when using a positive low pass filter K. This decomposition is then iteratively applied to the low resolution image yielding contrast coefficients C_k , $1 \le k \le N$ and a low resolution approximation L_N. An example of such a pyramid is displayed on Figure 2. This representation is easily inverted. Indeed consider the contrast coefficients $C_k(i,j)$ and low resolution $L_k(i,j)$. Using (5) a finer approximation of I can be computed as:

$$L_{k-1}(i,j) = ([L_k \uparrow 2] \star K(i,j)) \times \{C_k(i,j) + 1\} . \quad (6)$$

Applying this last equation iteratively as in Eq. 4 allows us to reconstruct I from its contrast coefficients.

2.2. QMF Pyramid Style

The next natural step is to address the problem of critically sampling the contrast representation. Many of the applications require critically sampled wavelet representations to

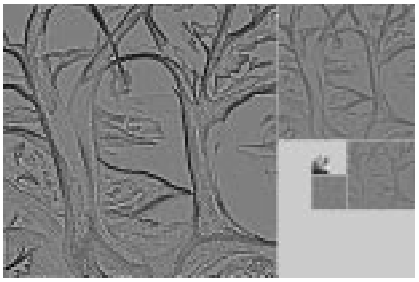

Figure 1: *Contrast pyramid of the test image.*

Figure 2: *Laplacian pyramid of the test image.*

eliminate redundancy. In our case, this is done by adapting the usual (bi-)orthogonal filterbank approach to wavelets. Let us consider the general case in which we have a pair of conjugate mirror filters (h, g) and their (bi-)orthogonal counterparts $(\tilde{h}, \tilde{g})$. At the analysis side, we use these filters to compute the usual three detail subbands D^h, D^v and D^d and approximation L. We then define three oriented contrast subbands by adaptatively normalizing the wavelet coefficients with L :

$$C^\lambda(i,j) = \frac{D^\lambda(i,j)}{L(i,j)} \;, \lambda = h,\, v,\, d\,. \tag{7}$$

The pyramid is constructed by cascading this operation to the low resolution approximation L. Let us now check that these coefficients are well defined for suitable analysis pairs (h, g). Let (ϕ, ψ) and $(\tilde{\phi}, \tilde{\psi})$ be the biorthogonal scaling functions and wavelets associated to these filters and let s be a positive definite square integrable function. Writing

$$\begin{aligned} \phi_{j,n}(t) &= \frac{1}{\sqrt{2}}\phi\big(2^{-j}t - n\big) \\ \psi_{j,n}(t) &= \frac{1}{\sqrt{2}}\psi\big(2^{-j}t - n\big) \end{aligned}$$

we have to ensure that

$$C(j,n) = \frac{\langle \psi_{j,n} | s \rangle}{\langle \phi_{j,n} | s \rangle}$$

is bounded. Using the two scale equations relating ϕ and ψ, we have

$$C(j,n) = \frac{\sum_k g_k^* \langle \phi_{j-1,2n+k} | s \rangle}{\sum_{k'} h_{k'}^* \langle \phi_{j-1,2n+k'} | s \rangle} \;. \tag{8}$$

By definition, the filter coefficients satisfy

$$g_k = (-1)^{1-k} \tilde{h}_{1-k}. \tag{9}$$

If we select positive low pass coefficients h_k, equations (8) and (9), together with the non-negativity of the signal, give a sufficient condition on the support of h and $\tilde{h}$:

$$\text{Supp}\left(\tilde{h}\right) \subseteq \text{Supp}\,(h) \;\;.$$

Obviously, many (bi-)orthogonal pairs satisfying these requirements can be found.

3. APPLICATION TO TRANSFORM CODING

The contrast normalized pyramids obtained for images are found to have useful properties for image processing applications. Consider the pyramid image of the “trees” test image obtained with the contrast normalization in Fig 1. It is clear that the detail images tend to have smaller values at higher scales, indicating that the increased number of decomposition levels reduces the dynamic range of the transform domain image. This property, which is not present in the regular Laplacian pyramid (Fig 2), may find useful applications in terms of compression.

Another useful property of the pyramidal decomposition is that the noise that can be added to the wavelet domain signals (during quantization) does not produce increased amount of noise variance in the reconstructed image. In other words, similar to the conventional pyramid case, the amount of noise added to the transform domain signal produces bounded and linearly proportional amount of noise in the reconstructed signal. This is important especially in the presence of noise introduced (e.g. by quantization) in the highest level (lowest detail). As an illustration, if the fourth level pyramid image is quantized to 32 levels, it produces a MSE of 7.63 in the reconstructed image, and if the third level pyramid image is quantized to 32 levels, the reconstructed image has a MSE of 7.64. Similar quantization of the first level produces a MSE of 7.70 in the reconstruction image. This indicates that the reconstruction error is linear with the quantization noise throughout the entire decomposition stages.

For the QMF style decomposition, the coders for wavelet trees have been extensively investigated [8, 9]. For this reason, we skip the quantization performance comparisons of contrast QMF with the regular QMF decomposition, and directly compare the coding performances with both objective and subjective quality criteria.

Image name	EZW PSNR	C-EZW PSNR
Lena_512	40.40	39.64
Baboon_512	29.35	28.42
Peppers_512	38.57	36.93
Barbara_512	36.28	34.98
Boat_512	36.57	35.55
Goldhill_512	36.53	35.73
Parrot_256	41.88	40.82

Table 1: Zerotree coding results at 1bpp

Consider the wavelet tree obtained by a contrast QMF in Fig. 3. The zerotree coders [8, 9] exploits the similarities along the different levels of decomposition corresponding to the same location of the image. In order to make the contrast pyramid compatible with the available coders, which are developed for coding wavelet tree outputs of regular QMFs (see Fig. 4), we applied a correction scale factor which is exponentially proportional to the level.

The test results in table 3 at 1 bits/pixel indicates very comparable PSNR performance of the contrast QMF with the original QMF. Furthermore, the images which have details at the dark areas give perceptually better reconstruction images at those portions. Better coders for the contrast QMF could possibly be obtained by considering the properties of the contrast pyramid instead of the regular wavelet pyramid. It has been demonstrated that, even with the tools that are ready at hand, one can obtain useful results using the new nonlinear contrast pyramid scheme. Investigation of other applications that may exploit the special properties of the contrast pyramid remains as an open direction.

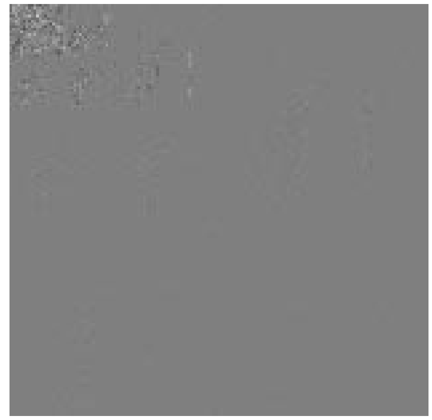

Figure 3: *Contrast wavelet tree of 'Lena' image.*

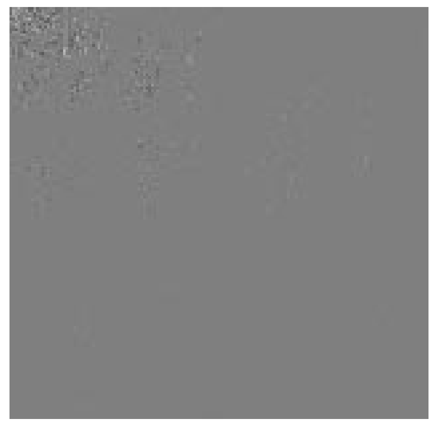

Figure 4: *Regular wavelet tree of 'Lena' image.*

4. REFERENCES

[1] J.-P. Antoine, R. Murenzi, B. Piette and M. Duval-Destin, "Image analysis with 2-D continuous wavelet transform: detection of position, orientation and visual contrast of simple objects," *Wavelets and Applications (Proc Marseille 1989)*, pp. 144-159, Y. Meyer (ed.), Masson, Springer-Verlag, 1992.

[2] S. Mallat and W.L. Hwang, "Singularity detection and processing with wavelets," *IEEE Trans. Inform. Theory,* **38** (1992) 617-643.

[3] M. Duval-Destin, M.A. Muschietti and B. Torresani, "Continuous wavelet decompositions, multiresolution and contrast analysis," *SIAM J. Math. Anal.* **24** (1993) 739-755.

[4] J.-P. Antoine and P. Vandergheynst, "Contrast enhancement in images using the two-dimensional wavelet transform," *Proc. 3rd International Workshop in Signal / Image Processing Advances in Computational Intelligence (IWSIP 96), Manchester*, Nov. 1996, pp. 65-68; B.G. Mertzios and P. Liatsis (eds.), Elsevier, Amsterdam 1996

[5] S. Winkler and P. Vandergheynst, "Local Contrast in Oriented Pyramid Decompositions," *in Proc. ICIP99, Yokohama, Japan, 1999*, submitted

[6] P. Burt and E. Adelson, "The Laplacian pyramid as a compact image coder," *IEEE Trans on Com.,* **31** 1983 482-540.

[7] E. Peli, Contrast in complex images, *J. Opt. Soc. Am. A,* **7***(10)*, 2032-2040, 1990.

[8] J. M. Shapiro, "Embedded Image Coding Using Zerotrees of Wavelet Coefficients," *IEEE Transactions on Signal Processing*, vol. 41, no. 12, pp. 3445 - 3462, Dec. 1993.

[9] Amir Said and William A. Pearlman, "An Image Multiresolution Re presentation for Lossless and Lossy Image Compression," *IEEE Transactions on Image Processing*, vol. 5, pp. 1303-1310, Sept. 1996.